ORNL/TM-2022/2384

Engineering Evaluation of Barium Buildup in a Decayed CsCl Sealed Source and Potential Impact for Cesium Release from a Breached Source

Charles F. Weber
David G. Abrecht

May 2022

OAK RIDGE National Laboratory

ORNL IS MANAGED BY UT-BATTELLE LLC FOR THE US DEPARTMENT OF ENERGY

ORNL/TM-2022/2384

Nuclear Nonproliferation Division

ENGINEERING EVALUATION OF BARIUM BUILDUP IN A DECAYED CsCl SEALED SOURCE AND POTENTIAL IMPACT FOR CESIUM RELEASE FROM A BREACHED SOURCE

Charles F. Weber
David G. Abrecht

May 2022

Prepared by
OAK RIDGE NATIONAL LABORATORY
Oak Ridge, TN 37831
managed by
UT-BATTELLE LLC
for the
US DEPARTMENT OF ENERGY
under contract DE-AC05-00OR22725

CONTENTS

LIST OF FIGURES

LIST OF TABLES

ACKNOWLEDGMENTS

This work was sponsored by the US Department of Energy, National Nuclear Security Administration, Office of Radiological Security.

ABSTRACT

For more than 50 years, radioactive ^{137}Cs has been a major source material for radioactive sealed sources, usually constructed as cesium chloride (CsCl) salt loaded into double-walled, stainless-steel capsules. A complication develops as ^{137}Cs decays to ^{137}Ba since this process creates a strongly reducing environment inside the capsule. A potential hazard exists if the capsule is breached and air ingress induces rapid exothermic oxidation, and this mechanism is suspected to be responsible for the well-known contamination incident at the Harbor View facility in Washington state. For this study, many thermodynamic evaluations were performed to assess the internal state of capsules after several decades of decay and to describe the potential oxidation if the capsule contents were to suddenly be exposed to air. Results suggest that reduction of impurities such as Cu, Fe, Pb, and Cr to metal will occur. If these impurities are lacking, it is possible that even Ba metal will form. In most cases, rapid oxidation can occur, and the exothermic reactions are sufficient to vaporize portions of the contents, which would include the remaining ^{137}Cs.

1. INTRODUCTION

One of the by-products of nuclear weapons production has been the generation of large amounts of high-level radioactive waste. It has been convenient to handle and dispose of this waste by separating out the highest-activity components, namely ^{137}Cs and ^{90}Sr. After such separations, the resulting elements could be stored as stable salts in secure and stable configurations. This was the goal of the Waste Encapsulation and Storage Facility (WESF) facility in Hanford, Washington.

More than 1,500 capsules containing cesium chloride (CsCl) were fabricated between 1974 and 1983 with the initial motivation of long-term storage [1]. Each capsule included a sizable inventory of ^{137}Cs and thus was highly radioactive. Over time, some of the capsules were appropriated for other purposes—namely for use as irradiation sources or as source material to fabricate radiation sources. However, most capsules were simply stored at the WESF facility in a secure and protected environment.

1.1 ACCIDENTS

Over the years, WESF capsules have experienced three notable failures. In 1988, one of several capsules used in a commercial irradiation facility began leaking and resulted in a contamination event that shut down the entire facility [2]. In 1990, the outer wall of a double-walled capsule failed at the WESF facility; fortunately, the interior wall remained intact and no radiation was released [3]. A third accident occurred in 2019 at the Harborview Research and Training Facility (HRT), which is operated by the University of Washington. This accident proved to have much more widespread consequences [4]. A thorough examination of the cause and the potential for other similar accidents is one of the primary motives behind the present study.

The HRT accident occurred when workers were attempting to cut open a CsCl source capsule with a high-speed cutting tool. Although the work was performed inside a portable hot cell, the progression of the accident resulted in the spread of radioactive material outside of the hot cell and contamination of several people. The apparent cause was vaporization of CsCl due to substantial heat generated during the operation, resulting in over-pressurization and failure of the hot cell. While some heat may have been due to the friction of the cutting operation itself, there was considerable suspicion that exothermic chemical reaction was involved when atmospheric O_2 entered the breached capsule. This study was designed to examine likely conditions and reactions that may have occurred, to provide guidance for subsequent handling and disposal operations for such sources.

1.2 GOALS OF THIS PROJECT

Numerous previous studies have reported measurements of capsule contents, and researchers have hypothesized the possible chemical reactions that could occur over many decades of source lifetimes. Many of these features are summarized in Section 2, in which variations in impurity contents as well as CsCl isotopics are noted. Both features strongly affect the expected conditions inside the capsules.

One of the goals of this work was to make quantitative calculations of the capsule internal chemistry to understand more thoroughly the HRT accident and the general risks posed by handling and disposal of similar capsules. The internal chemistry is complicated by the decay of ^{137}Cs to ^{137}Ba, which gradually creates reducing conditions inside the capsules. Such calculations have been performed using the FactSage code for chemical equilibria [5], and the calculations are described in Sections 3 and 4.

A second question to be addressed in this study is the possibility of radiation release or a contamination event such as HRT. Given the conditions inside a capsule, would exposure to air promote rapid exothermic reaction sufficient to vaporize some of the contents? This question will also be addressed by thermodynamic equilibrium calculations, even though to be fully understood would require a transient kinetic analysis. This question is discussed briefly in Sections 2 and 3 but evaluated more fully in Section 4.

2. CsCl CAPSULES

2.1 CSCL DECAY EFFECTS

The Cs isotopes in the capsules are fission products formed in nuclear reactors and comprise three principal isotopes: stable ^{133}Cs, nearly stable ^{135}Cs, and ^{137}Cs (half-life 30.2 years[1]). Other isotopes may have been present at one time but have decayed sufficiently to be insignificant. The ^{137}Cs continues to decay to ^{137}Ba, but the resulting chemical forms may not be chlorides and likely depend on many other constituents that may be present. In the case of a sealed container, such as the WESF capsules, reducing conditions ensue and an ion imbalance results since insufficient Cl exists to form the preferred species $BaCl_2$. In the nominal case where ^{137}CsCl decays in the complete absence of oxidizing materials or impurities, both $BaCl_2$ and Ba metal are likely to form:

$$2CsCl \xrightarrow{\beta-} 2Ba^{2+} + 2Cl^{-} \rightarrow BaCl_2 + Ba. \quad (1)$$

Under this scenario, Ba metal would continue to accumulate as ^{137}Cs decays, creating highly reducing conditions after many decades. Because ^{135}Cs has a long half-life, it does not decay significantly over the expected lifetime of the capsules and does not contribute to this effect.

One report [6] notes that CsCl has a theoretical density of 3.97 g/cm^3; however, methods of construction suggest that this density is never reached. Some sources are constructed of cold-pressed CsCl powder, which has a maximum practical density of 3.3 g/cm^3. As a safety measure to allow for the expansion of a crystalline phase change of CsCl at 460°C, most such sources are pressed only to 2.5 g/cm^3. The WESF capsules are filled with molten CsCl that shrinks on cooling, inducing cracking and other disruption.

[1] All calculations in this paper were done using the 2006 assessment that ^{137}Cs half-life is 30.2 years. More recent assessments have recommended a slight modification of 30.1 years. This distinction is not significant in the calculations performed or the conclusions of this work.

Thus, the original material is not highly confined, but it may allow some migration and interaction. Additionally, there will be some interstitial space occupied mostly by gas molecules.

Concern exists that if the interstitial space were occupied by air, then O_2 would interact with the source material and could have a significant effect on the chemistry of the source as radioactive decay occurs. The O_2 would form a buffer of sorts through the reaction:

$$2\mathrm{CsCl} \xrightarrow{\beta-} 2\mathrm{Ba}^{2+} + 2\mathrm{Cl}^{-} \xrightarrow{\mathrm{O_2}} \mathrm{BaCl_2} + \mathrm{BaO}. \tag{2}$$

However, the manufacturing process for most sources includes welding the inner capsule shut under an inert gas atmosphere (He or Ar), which suggests that no significant quantity of O_2 is present in the sealed capsule.

Other researchers have conducted a theoretical analysis using density functional theory [7, 8], which indicates that when ^{137}Cs decays to ^{137}Ba, the resulting Ba can form metastable BaCl that may remain in the rock salt lattice with CsCl. These authors note that this form of barium chloride is unstable, and that the phase separation to $BaCl_2$ + Ba(s) is thermodynamically preferred. However, they maintain that the instability is small and the driving force for phase separation is only 0.03 eV/atom. These authors note that their analysis has ignored any driving force due to e^- recoil, gamma radiolysis, or other kinetic effects. Furthermore, they do concede that the BaCl species has never been observed experimentally. Whether the source material is metastable BaCl or $BaCl_2$ and Ba metal, air ingress would presumably produce rapid oxidation in either case. A preliminary thermodynamic analysis of these two scenarios at T = 300 K produces:

$$\mathrm{BaCl_2} + \mathrm{Ba(s)} + \frac{1}{2}\mathrm{O_2} \rightarrow \mathrm{BaCl_2} + \mathrm{BaO}, \quad \Delta H = -907.885\ \mathrm{kJ}, \tag{3a}$$

$$2\ \mathrm{BaCl} + \frac{1}{2}\mathrm{O_2} \rightarrow \mathrm{BaCl_2} + \mathrm{BaO}, \quad \Delta H = -1{,}122.085\ \mathrm{kJ}. \tag{3b}$$

Therefore, if Ba does not phase separate but remains as metastable BaCl, then even greater heat is released, producing a greater potential hazard. Hence, reaction (3a) is bounding, in that if it results in serious consequences, then a scenario under Eq. (3b) would as well. Of course, the kinetics of these reactions have not been considered, as this study is based wholly on equilibria.

Lamb's study [6] mentions that metallographic examination of a 2.5 year old source indicated penetration of only 25–75 μm (1–3 mils) of source material into the cladding (316 SS), which does not appear to be substantial. If any reactions take place involving the capsule material, it would be important to consider.

2.2 CAPSULE COMPOSITION.

Numerous reports have examined the impurity content of WESF Cs capsules [1, 9, 10, 11, 12, 13, 14, 15]. Most of these publications have ventured some explanation or calculation of thermodynamic effects of impurities, primarily out of concern for the possible impact on corrosion of the inner capsule. However, these studies generally indicate that impurities tend to inhibit corrosion. In addition, they also tend to ameliorate the effects of the reducing atmosphere due to the decay of Cs to Ba. The mechanism posited to explain this phenomenon is that Ba metal has higher oxidation potential than most of the impurity metals; hence, the Ba will preferentially extract chloride from the impurities and, if any metal forms, it will likely be Fe, Cu, Pb, or other impurity metals instead of Ba. In at least one study, this mechanism is suggested to

help regenerate chloride corrosion species in the capsule wall and slow corrosion rates [11]. Of course, the thermodynamic analysis does not ensure that kinetics and transport are favorable and the preferred metals actually do form. Nevertheless, many years of operation and estimated storage temperatures in the range of 200°C to 400°C suggest that the thermodynamic analysis is a good estimator.

More than a dozen measurements have been taken by multiple analytical teams at several different laboratories. Some of the impurity contents vary widely, due in part to the varying content of different capsules. However, considerable variation also exists in the analytical capabilities and techniques that contribute to uncertainties in impurity contents. Therefore, it must be recognized that each impurity element has a distribution of possible values. For example, Table 1 lists values obtained from 17 different measurements of sodium (as NaCl). These values are ordered and grouped into general classes denoted in the first column.

Table 1. NaCl impurity measurements (wt% NaCl).

General group	Experimental measurements						
≤ 0.1	0.04	0.1	0.1	0.1			
0.1 – 0.5	0.18	0.2	0.2	0.3	0.3	0.3	0.3
0.5 – 2	0.7	0.7	1.5				
> 2	2.8	4.5	7.76				

The references from which these are obtained seem to indicate that these are independent measurements. However, indefinite descriptions allow some possibility that some of these values are duplicates of each other, drawn from the same sources. Furthermore, there is no assurance that the measurements were intended as random samples to describe the entire population of WESF capsules. Rather, the particular capsules were chosen for convenience because they were readily available or researchers had some other motivation for examining them. Nevertheless, in this study, the authors will assume that the measurements obtained are representative of the WESF capsule population, and that statistical distributions of impurities can be inferred from them.

A crude distribution for NaCl can be ascribed by assigning each row in Table 1 into a histogram category. The resulting distribution is plotted in Figure 1 and can be regarded as a probability density for NaCl impurity. Of course, construction of such a distribution involves some assumptions, such as the location of region boundaries, but it does reflect the principal features of NaCl in WESF capsules.

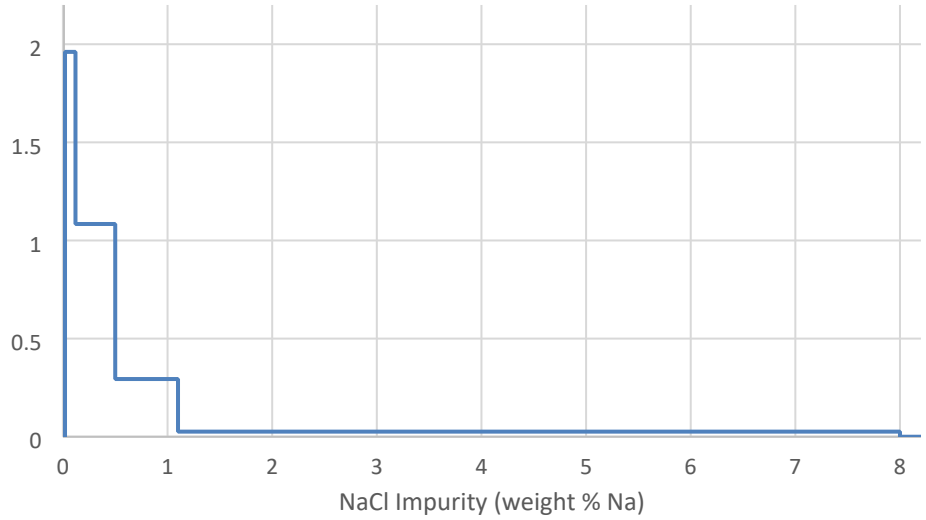

Figure 1. Statistical distribution of Na impurity (wt% cation).

An alternate approach is taken by Storch's study [1], which provides an assessment of impurities and gives a recommended value and a maximum. This report's preferred values are shown in Table 2 and will be used to construct a prototype capsule. (Minor impurities, which are recorded for only a few capsules, and are present in very small amounts, are omitted.) Note that only cation impurities are given in Table 2, and Cs and Ba are omitted. The likely species are given in the fourth and eighth columns and are assumed to involve only Cl and O in addition to the cations. The manufacturing process suggests that most species are chlorides, but Al and Si are likely due to trace contamination from purification in zeolite ion exchange, and are therefore assumed to be oxide. In addition, no solid chloride of B is known, so it also is assumed to be oxide. Thus, the list represents the initial inventories before any decay to Ba occurs. Barium is assumed to be fully removed in the cesium separation process before loading the capsules, so the initial content of barium is assumed to be zero. The value of Cs is assumed to be the balance after consideration of all the elements in Table 2, including Cl and O.

Table 2. Impurities summarized by Storch [1]. Values shown are cation wt%.

Element	Preferred	Maximum	Species		Element	Preferred	Maximum	Species
Al	0.7	1.5	Al_2O_3		Mo	0.06	0.06	$MoCl_5$
B	1	2.58	B_2O_3		Na	2	7.32	NaCl
Ca	0.2	2.77	$CaCl_2$		Ni	0.5	0.73	$NiCl_2$
Co	0.22	0.22	$CoCl_2$		Pb	1	1.88	$PbCl_2$
Cr	1	4.27	$CrCl_3$		Rb	0.7	0.7	RbCl
Cu	0.31	0.31	CuCl		Si	0.9	0.9	SiO_2
Fe	1.14	1.14	$FeCl_2$		Sr	0.33	0.33	$SrCl_2$
K	1.51	1.51	KCl		Ti	0.17	0.17	$TiCl_4$
Mg	0.5	0.98	$MgCl_2$		Zr	0.2	0.2	$ZrCl_4$
Mn	0.11	0.11	$MnCl_2$					

For the preferred capsule in [1], the total constituents are given in Table 3.

Table 3. Total composition of prototype capsule (wt%).

Element	Typical
Cs	56.04
Cl	27.54
O	3.87
Other[a]	12.55

[a] Cation impurities from Table 2.

Only one reference [12] evaluates the gas phase contents of a capsule, and this is only performed for one capsule. Thus, unlike the solid salt impurities, only one sample for the gas content of the capsules exists, Capsule C-117, which holds a total salt content of 2.708 kg [1]. The gas inventories are given by volume (cm^3), then converted to total mass inventories in the entire capsule. Typical values for solid components can also be converted to total capsule inventories representative of capsule C-117 by multiplying weight percents by 27.08, and values for all constituents are given in Table 4. These will be used as best estimates for initial calculations that include gaseous constituents.

Table 4. Total molar inventories of a hypothetical capsule.

Solid species [a]						Gaseous species [b]	
Element	**mol**	**Element**	**mol**	**Element**	**mol**	**Element**	**(mmol)**
Cs	11.286	Co	0.101	Na	2.356	H_2	0.00094
Cl	21.170	Cr	0.521	Ni	0.231	He	1.058637
O	11.36	Cu	0.132	Pb	0.131	CH_4	0.000245
Al	1.406	Fe	0.553	Rb	0.222	H_2O	0.002861
B	5.01	K	1.046	Si	0.868	N_2+CO	0.465964
Ba[c]	0.000	Mg	0.557	Sr	0.102	O_2	8.17E-05
Ca	0.135	Mn	0.054	Ti	0.096	Ar	0.768431
		Mo	0.017	Zr	0.059	CO_2	0.001144

[a] Taken from Storch [1].
[b] Taken from Kenna [12].
[c] Values will grow in over time.

2.3 CESIUM DECAY AND BARIUM BUILDUP

Many authors have measured Cs isotopics for one or more capsules, usually determined by inductively coupled plasma mass spectrometry. Assuming that no Ba is present initially, the ^{137}Ba is included in the ^{137}Cs value. Hence, the measurements do not reflect nor are they affected by the decay of ^{137}Cs.

Storch [1] gives measurements of Cs isotopes for 24 canisters, with the mean and standard deviations given in Table 5. The most predominate isotope is ^{133}Cs, and its value was obtained by subtracting values for the other isotopes from 100. The values for ^{137}Cs are clustered around 32%. A few reports give very small inventories of ^{134}Cs, but this isotope is largely inconsequential since, with a half-life of 2.1 years, it has largely decayed away before the capsules were even filled. Also shown in Table 5 is the average atomic weight for Cs based on this distribution of isotopes.

Table 5. Cesium isotopes (mol%).

	Mean (mol%)	Standard deviation (mol%)
^{133}Cs	53.9	2.38
^{135}Cs	14.05	1.73
^{137}Cs	32.05	1.63
Atomic weight	134.4691	4.52

The decay of ^{137}Cs has a half-life of 30.2 years, which translates to a decay constant of $\lambda = 0.02295\ \mathrm{y}^{-1}$. Over time, the inventory of ^{137}Cs follows the standard equation

$$N(t) = N(0)e^{-\lambda t}\,, \tag{4}$$

where $N(0)$ is the initial inventory (mol) of ^{137}Cs, and $N(t)$ is the amount after t years. Of course, the decrease in ^{137}Cs is matched exactly by an increase in ^{137}Ba inventory. Table 6 shows this reduction of Cs and increase of Ba over time. Note that the Cs column contains all isotopes, whereas the Ba column is composed only of ^{137}Ba.

Table 6. Cesium decay and barium ingrowth.

	Molar inventories	
Time (y)	Cs	Ba
0	11.28559	0
5	10.90046	0.385138
10	10.55708	0.72852
15	10.25093	1.034673
20	9.97797	1.307633
25	9.734606	1.550998
30	9.517628	1.767979
35	9.324175	1.961434
40	9.151695	2.133915
45	8.997916	2.287695
50	8.86081	2.424803

3. CHEMICAL EQUILIBRIUM CALCULATIONS

As mentioned in the introduction, one of the purposes of this study was to understand the conditions inside CsCl sealed sources, especially as ^{137}Cs decay occurs and the reducing conditions unfold. We have examined the contents of typical capsules, including impurities, Cs isotopics, and the decay over time. The authors recognize that many parameters are not known exactly but can be characterized using statistical distributions obtained from measurements. In this section, capsule contents are described using chemical equilibrium calculations. This process does not ensure which species are actually present, but it does give a sense of the likely composition. A sample calculation is described in Section 3.1, and a Monte Carlo sampling scheme is outlined in Section 3.2 that illustrates a variety of possible conditions and their uncertainties.

3.1 STANDARD EQUILIBRIUM CALCULATION

The molar inventories in Tables 4 and 5 are used as input to an equilibrium calculation using the FactSage code [5]. As an example calculation for decay of 40 years, the appropriate line is chosen from Table 6 for the Cs and Ba inventories together with all of the other impurity values from Table 4. Each cation is input as either a chloride or oxide (see Table 1), so it is unnecessary to input Cl and O as individual elements. Results for a calculation at 400 K are shown in Table 7. The first three pairs of columns represent solid phase species, and the last pair of columns represent gas phase species.

Table 7. Chemical equilibrium in a prototype CsCl capsule.

Species	mol	Species	mol	Species	mol	Species	mol
CsCl	7.801	Cs_2MgCl_4	0.557	Co_2B	0.0505	He	0.001059
NaCl	2.356	$CsCaCl_3$	0.135	Cu	0.132	Ar	7.68E-04
$BaCl_2$	2.1339	$CsSrCl_3$	0.102	$KMnCl_3$	0.054	H_2	1.77E-06
B_2O_3	2.0576	K_2FeCl_4	0.3735	Ni	0.0991	CH_4	1.26E-06
SiO_2	0.809	$(Al_2O_3)_2(B_2O_3)$	0.3515	$ZrSiO_4$	0.059		
$CrCl_2$	0.521	$TiCl_3$	0.0067	$Ti_{10}O_{19}$	0.0089		
RbCl	0.222	$KFeCl_3$	0.1795	Mo_2B	0.0085		
NiB	0.132	KPb_2Cl_5	0.0655	BN	9.32E-04		
				Mo_2C	1.26E-07		

Note that Ba exists only as $BaCl_2$, having scavenged Cl atoms from some of the metal impurities. As a result, some of these impurities exist as pure metals (Cu, Ni) or as reduced compounds not involving Cl (NiB, Co_2B, Mo_2B, BN, Mo_2C). A number of multi-cation salts seem to be thermodynamically favored (e.g., Cs_2MgCl_4), but these do not change the overall stoichiometry of the system [Cs_2MgCl_4 = $(CsCl)_2 \cdot MgCl_2$] or the association of Cl atoms. Also of note is the slight reduction of Ti from $TiCl_4$ to $TiO_{1.9}$.

3.2 MONTE CARLO SAMPLING: VARIABILITY AND UNCERTAINTY

The results in Table 7 are quite informative, but only involve a single capsule composition, namely that of a prototype capsule described by Tables 4 and 5. Many capsules might deviate considerably from this typical example, and the analysis in this section is designed to capture the variability in capsule behavior that may be possible. It is based on the observation that many of the parameters, including impurity contents and Cs isotopics, can vary widely. The analysis in this section describes variability for 100 g of material in a WESF capsule.

To begin, we revisit the distribution of NaCl impurities in WESF capsules described in Table 1 and Figure 1. For each impurity in Table 2, such distributions are constructed, as described fully in Appendix A. For most of the impurities, the measurement data are not as extensive as for NaCl, but the data are still sufficient to provide crude histograms for statistical distributions. Using a computer calculation with a random number generator, these distributions can be sampled, thereby constructing a wide variety of capsules that can be analyzed.

The analysis described here is conducted as follows:

1) For each element in Table 2, take a random sample from its statistical distribution and assign it as the inventory of that element in a capsule.

2) Take a random sample from the Cs isotopic distribution in Table 5 by assuming it has a normal distribution.

3) Introduce variability into the gas phase composition by taking a random sample from a normal distribution with mean from the last column of Table 4 and standard deviation of 10% of the mean.

4) Decay the ^{137}Cs for 45 years according to Eq. (4).

Performing the above steps creates a random sample that in some ways represents contents of a hypothetical capsule after 45 years. Conducting many such samplings represents the variability that could be encountered by sampling many actual capsules. The basis for these results is 100 g of capsule contents.

Such a sampling analysis produces results that are expected and some which are surprising. The variability in impurity content (both solid and gaseous) produces a wide variety of redox conditions, and therefore a variety of equilibrium species. Table 8 shows a listing of the Al, Cs, and Ba species that were obtained in at least one of the hypothetical capsules. It is not surprising that Al includes many oxide species since it is one of the primary sources of oxygen in the capsule, together with Si and B. Recall that the Al and Si impurities are largely assumed to be remnants of the zeolite used in the ion exchange purification immediately before molten CsCl is poured into the capsule. The B impurity is commonly found in a number of other elements. It is noteworthy that both Al and Ba occur as reduced species including as pure metals (AlN, Al, Ba_3N_2, Ba, BaH_2, Ba_2Pb). However, note that the reduced Ba species are rare, with $BaCl_2$ being the overwhelmingly dominant species. For Cs, all of the compounds are associations of standard chloride or oxide species. Similar lists could be constructed for all other elements in Table 2 and would also illustrate a wide variety of compounds, many of which were in a reduced state.

Table 8. Equilibrium species for Al, Cs, and Ba.

Al Species	Cs Species	Ba Species
$(Al_2O_3)_2 \cdot (B_2O_3)$	$CsCl$	$BaCl_2$
$BaO \cdot (Al_2O_3)$	$CsCaCl_3$	$(BaO) \cdot (TiO_2)$
$(BaO)_3 \cdot (Al_2O_3)$	Cs_2MgCl_4	$(BaO) \cdot (ZrO_2)$
Al_2SiO_5	$CsBO_2$	$(BaO) \cdot (SiO_2)$
$(Al_2O_3)_9 \cdot (B_2O_3)_2$	Cs_2ZrO_7	$(BaO) \cdot (SiO_2)_2$
AlN		$(BaO)_2 \cdot (SiO_2)$
Al		$(BaO) \cdot (Al_2O_3)$
Al_4Sr		Ba
Al_3Ni		Ba_2Pb
		Ba_3N_2
		$(BaO)_3 \cdot (Al_2O_3)$
		BaO
		BaH_2

3.3 EXPOSURE TO AIR

If the capsule is breached, air ingress can result in oxidation of several species, most notably the metals and reduced species in Tables 7 and 8. To simulate this action, the species in Table 7 are combined with an excess of $O_2 + N_2$ and a new equilibrium is calculated. All results presented here combine 20 mol N_2

and 5 mol O_2 with the species in Table 7 or one of the cases described in Section 3.2. Table 9 shows the results of both equilibrium steps at 400 K for the prototype capsule represented by Table 7. For ease of comparison, the first pair of columns are the species input to the initial equilibrium calculation (which includes the unstable form BaCl) from Tables 4–6. The second pair of columns are the results of the equilibrium calculation for the enclosed capsule, identical to Table 7. In the last pair of columns, all cations are fully oxidized, as would be expected on exposure to air. Volatilization of several components occurs, so a sizable inventory of Cl_2 and HCl exists in the gas space, as well as small amounts of metal chlorides and oxychlorides.

Table 9. Prototype capsule exposed to air.

Nonequilibrium Input			Equilibrium Calculation			Exposed to Air	
Species	**mol**		**Species**	**mol**		**Species**	**mol**
CsCl	9.151695		CsCl	7.9126		CsCl	8.5909
B_2O_3	2.505		B_2O_3	1.9228		NaB_5O_8	0.2586
			BN	9.32E-04			
NaCl	2.356		NaCl	2.356		NaCl	2.0974
BaCl	2.133915		$BaCl_2$	2.1339		$BaCl_2$	2.1339
KCl	1.046		K_2FeCl_4	0.3735		KCl	0.397
SiO_2	0.868		SiO_2	0.809		SiO_2	0.809
Al_2O_3	0.703		$(Al_2O_3)_2(B_2O_3)$	0.3515		$(Al_2O_3)_2(B_2O_3)$	0.3515
$MgCl_2$	0.557		Cs_2MgCl_4	0.50104		MgB_4O_7	0.557
			MgB_4O_7	0.055958			
$FeCl_2$	0.553		$KfeCl_3$	0.1795		Fe_2O_3	0.2765
$CrCl_2$	0.521		$CrCl_2$	0.521		$Cs_2Cr_2O_7$	0.2095
$NiCl_2$	0.231		NiB	0.17765		$KniCl_3$	0.231
			Ni	0.05335			
RbCl	0.222		RbCl	0.222		RbCl	0.222
$CaCl_2$	0.135		$CsCaCl_3$	0.135		$CsCaCl_3$	0.135
$CuCl_2$	0.132		Cu	0.132		$CuCl_2$	0.132
$PbCl_2$	0.131		KPb_2Cl_5	0.0655		PbB_6O_{10}	0.131
$SrCl_2$	0.102		$CsSrCl_3$	0.102		$SrCrO_4$	0.102
$CoCl_2$	0.101		Co_2B	0.0505		K_2CoCl_4	0.101
$TiCl_2$	0.096		$Ti_{10}O_{19}$	0.0096		TiO_2	0.096
$ZrCl_4$	0.059		$ZrSiO_4$	0.059		$ZrSiO_4$	0.059
MnCl2	0.054		$KMnCl_3$	0.054		$K4MnCl_6$	0.054
MoCl2	0.017		Mo_2B	0.008496		$Cs_2Mo_5O_{16}$	0.0034
			Mo_2C	1.26E-07			
He	1.06E-03		He	0.001059		He	0.001059
Ar	7.68E-04		Ar	7.68E-04		Ar	7.68E-04
N_2+CO	4.66E-04					N_2	20
H_2O	2.86E-06					O_2	3.0572
CO_2	1.14E-06					Cl_2	1.9467

Table 9. Prototype capsule exposed to air (continued).

Non-equilibrium Input			Equilibrium Calculation			Exposed to Air	
Species	**mol**		**Species**	**mol**		**Species**	**mol**
H_2	9.40E-07		H_2	1.77E-06		HCl	8.27E-06
CH_4	2.45E-07		CH_4	1.26E-06		CO_2	1.39E-06
O_2	8.17E-08					CrO_2Cl_2	8.38E-07
						$CrOCl_3$	2.16E-07
						H_2O	1.53E-07
						$PbCl_4$	1.50E-07

3.3.1 Enthalpy changes

One of the principal questions motivating this study was the possibility that excess heat would be generated by air oxidation and that this might volatilize some of the remaining CsCl in the capsule. For the prototype case in Table 9, the reaction due to air oxidation yields an enthalpy change calculated as follows:

$$\Delta H = H_0 - \left(H_{\text{cap}} + H_{\text{air}}\right), \tag{5}$$

where $H_0 =$ total enthalpy of the system after reaction with excess air,
$H_{\text{cap}} =$ enthalpy of the capsule at equilibrium after 40 years decay, and
$H_{\text{air}} =$ enthalpy of the excess air (20 mol N_2 + 5 mol O_2).

At 400 K, H_{air} is calculated as follows from values for N_2 and O_2 in Ref. [16]:

$$H_{\text{air}} = 20\ [\text{mol}] \times 2{,}971 \left[\frac{\text{J}}{\text{mol}}\right] + 5[\text{mol}] \times 3{,}029 \left[\frac{\text{J}}{\text{mol}}\right] = 74{,}430\ \text{J}\,.$$

For the prototype capsule reflected in Table 9, the enthalpy change was: $\Delta H =$ -1.56E5 J. This is sufficient to vaporize at least some of the capsule contents, which still contain enough ^{137}Cs to produce a serious contamination accident.

For each of the hypothetical cases in Table 8 (for 100 g of capsule material), an equilibrium calculation (at constant pressure and temperature) was also performed to simulate reaction with excess air. Each of these cases produced fully oxidized constituents very similar to the last pair of columns in Table 9. Because of the wide variability in the reduced species in the capsule materials, the enthalpy changes also reflected wide ranges. Results are shown in Table 10 and indicate that the reaction is exothermic in every case. These values range between 14.253 kJ $\leq -\Delta H \leq$ 49.212 kJ and can be ordered and used to derive a cumulative distribution of ΔH values. This distribution is illustrated in Figure 2 and has a mean of $\overline{\Delta H}$ $= -$ 24.6 kJ and a standard deviation of 8.8 kJ.

Table 10. Enthalpy changes (J) in 100 g of hypothetical capsule contents exposed to air at 400°C.

-16152	-27045	-28294	-17533	-17509
-21134	-41999	-15871	-21229	-18342
-20780	-21851	-32951	-44017	-15111
-31792	-16076	-27190	-18731	-19655
-30923	-14253	-18191	-42667	-20792
-15225	-17332	-30085	-27903	-20461
-25591	-32669	-14286	-18408	-21986
-19944	-49212	-34978	-39985	-18851
-21265	-28594	-41766	-20002	-31830
-20187	-15471	-16963	-31441	-20097
-21077	-17509	-21614	-17191	-28294
-17508	-18342	-18230	-20345	-15871
-17186	-15111	-19658	-40370	-32951
-15364	-19655	-45867	-24964	-27190
-31797	-20792	-21062	-40956	-18191
-23466	-20461	-18793	-17332	-30085
-19905	-21986	-36996	-32669	-14286
-17788	-18851	-25441	-49212	-34978
-28367	-31830	-20436	-28594	-41766
-36279	-20097	-23340	-15471	-16963

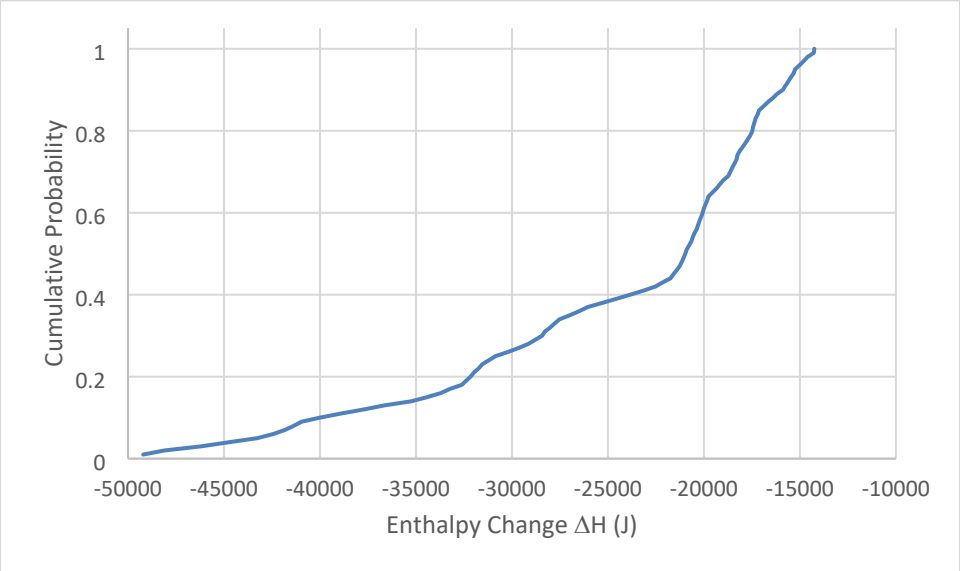

Figure 2. Cumulative distribution of enthalpy changes for 100 g of capsule contents.

The exothermic nature of the reaction with air again indicates the possibility that enough heat is available to vaporize some of the contents of the capsule, including any ^{137}Cs that might still remain.

4. SENSITIVITY ANALYSIS

In addition to understanding the behavior of the enthalpy of representative capsules, this work attempted to understand the effect of variations of the typical range of impurities, the isotopic concentration of the Cs, and the storage temperature on the maximum achievable temperature and vapor concentration of Cs caused by oxidation of the reduced system. The base case for the calculations was represented by the values of isotopics and impurities shown in Tables 4 and 5, with a storage temperature of 168.5°C. This temperature represents the ideal gas temperature taken from the pressure and volume values obtained from the gas analysis of capsule C-117 and was considered indicative of the internal gas temperature in contact with the CsCl salt [12]. Calculations were performed to evaluate a set of four storage temperatures (T = 25°C, 72.83°C, 120.67°C, and 168.5°C), a set of four ^{137}Cs compositions representative of the ranges provided in the report by Storch (30%, 32%, 34%, and 36%, with the balance stable ^{133}Cs) [1], and variations of individual impurities across their expected ranges, as provided in Appendix A. The value of a single impurity was altered one at a time for the impurity calculations. However, maintaining a consistent anion balance (Cl, O) required altering the amount of CsCl and other impurities present in the system. These values were adjusted accordingly to maintain charge balance. A full list of the conditions used for the sensitivity analysis is given in Appendix B.

The procedure for the calculations is essentially the same as that performed in Section 3, except for a few minor variations. Instead of a single age for the capsule, the set of capsule components were calculated yearly for ages 0 to 81 years, representing the entire design lifetime of the capsules [3] and the corresponding in-growth of decay Ba. As in the calculations in the previous section, the initial list of capsule contents for the calculation was isothermally equilibrated under reducing conditions, then isothermally oxidized with excess dry air at atmospheric pressure and the same storage temperature to obtain the change in enthalpy from the oxidized system and the amount of oxygen consumed by the oxidation reaction at completion. To ensure an excess, the amount of air used was increased to 50 moles of O_2 and 238.1 moles of N_2, and N_2 was treated as inert in all calculations. Because the unreacted air is incorporated in both the “total system enthalpy” and in the “enthalpy of air” component of Equation 5, the additional unreacted air will not affect the calculation of the change in enthalpy because of the oxidation. As a final step in the sensitivity analysis, an additional calculation was performed in which the amount of O_2 reacted to achieve equilibrium in the oxidation reaction was used to obtain a new mass of dry air at atmospheric pressure and the storage temperature. This was added to the initial calculation concentrations used for equilibrating the reduced system (i.e., the starting capsule concentrations). The entire system was then adiabatically equilibrated, using the change in enthalpy previously calculated to determine a final maximum temperature and concentration of ^{137}Cs species in the vapor phase.

4.1 EFFECTS OF STORAGE TEMPERATURE

Changes due to the initial storage temperature had a predictable behavior, with maximum oxidation temperature and ^{137}Cs species vapor pressure showing increases with increased starting temperature. Figure 3 and Figure 4 show the effect of age and storage temperature on these variables. Even though the full range of chemical species was available in the gas phase, the dominant chemical species of ^{137}Cs in the vapor phase were $^{137}CsCl$ and $(^{137}CsCl)_2$ dimer, indicating that the vaporization is primarily dominated by heating effects and not by the formation of uniquely volatile compounds. This relationship held true for all of the sensitivity studies and suggests that the achieved temperature is the dominant driver for volatilizing the Cs from these capsules, with the effect of impurities and age only modifying the behavior through their role in altering the system temperature. This effect is further observed by plotting the log of the Cs vapor concentration against the inverse of the temperature, shown in Figure 5, which depicts the classic exponential relationship expected from vaporization.

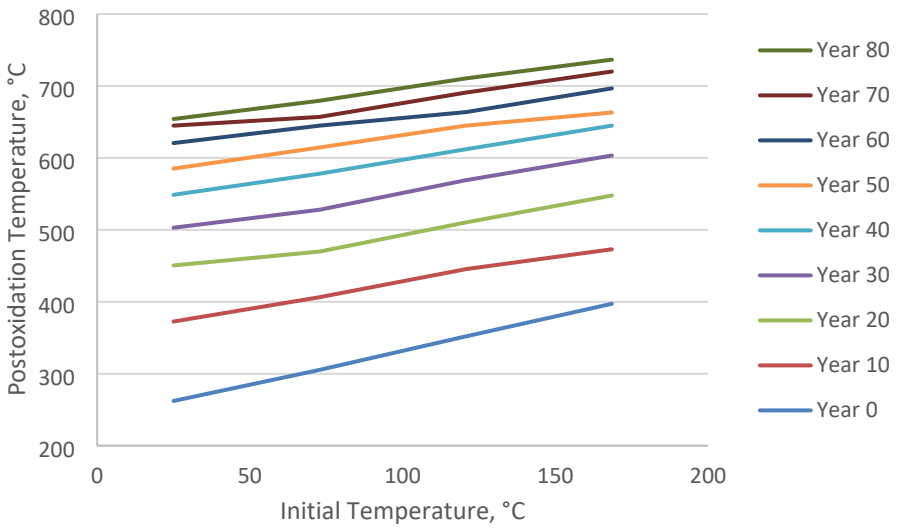

Figure 3. The effects of age and initial storage temperature on the maximum adiabatic postoxidation temperature achieved due to oxidation. Even before any decay Ba is produced (Year 0), the potential for large amounts of heat generated from the formation of impurity oxides is possible.

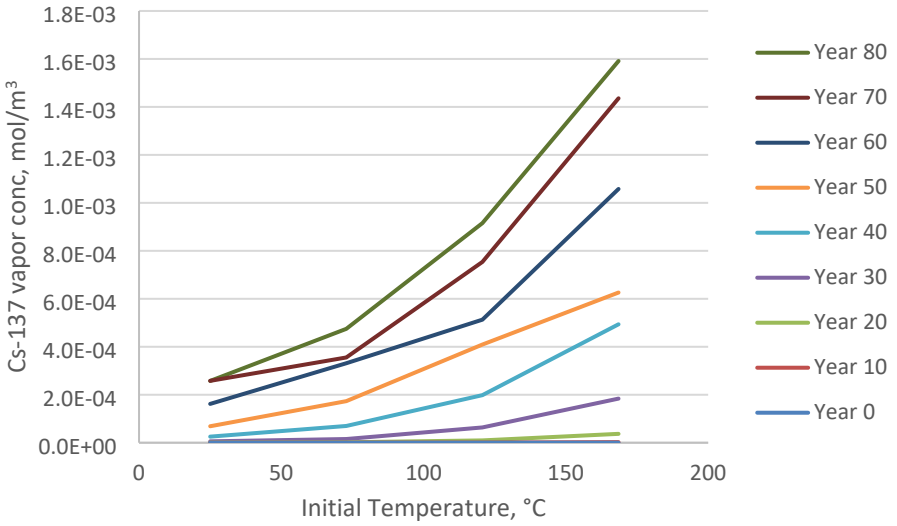

Figure 4. Cesium-137 vapor concentration from thermodynamic equilibrium calculations as a function of age and initial storage temperature.

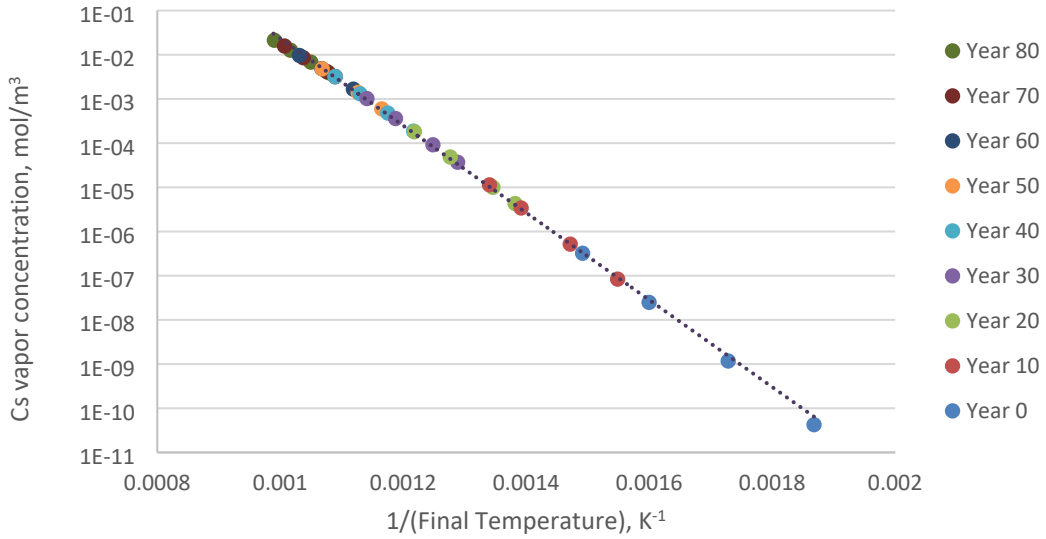

Figure 5. Plot of Cs vapor concentration against inverse temperature, showing the classic exponential dependence of the vapor pressure.

The results of the thermodynamic analysis indicate that the sudden oxidation of the CsCl salt bed has the potential to create significant amounts of heat, raising the temperature by several hundred degrees. Even before any decay of ^{137}Cs (represented as Year 0 in the following figures), the instability of chloride impurities generated significant exothermic reaction with atmospheric oxygen. That is, exothermic reaction of Fe, Ti, Mo, Cr and other chlorides with O_2, and the formation of secondary impurities such as MgB_4O_7 generate significant heat and release significant amounts of chlorinated gaseous products. In reality, these behaviors are likely to be heavily kinetically limited and/or to occur to some extent spontaneously before sealing the capsule, so their effects are likely not as significant as indicated by the equilibrium models. However, the thermodynamic potential for these effects to occur represents a potential heat load for the system.

As the system increases in age from Year 0, Figure 3 shows that a flattening occurs in the effect of the storage temperature on the final achievable temperature, and there are distinct "kinks" in the temperature curves at approximately 470°C and 644°C. These kinks represent that part of the heat released by oxidation is absorbed by a solid-solid phase change in CsCl and the melting of CsCl, respectively. These phase changes produce the flattening effect that reduces the slope of the final achieved adiabatic temperature as a function of initial storage temperature.

4.2 EFFECT OF CS ISOTOPICS

The relative amount of ^{137}Cs was varied between 30% and 36% to identify the effect of Cs isotopics on the achieved adiabatic final temperature and ^{137}Cs vapor content. Again, the results were predictable. At Year 0, the isotopic concentration had no effect on the system behavior because no decay had yet occurred. As the capsule age increased, the increased amount of ^{137}Cs led to increased amounts of ^{137}Ba, leading to a higher oxidation potential and higher final temperatures and vapor concentrations (Figure 6 and 7). At the very highest concentration of 36% ^{137}Cs, a crossover point was achieved, where sufficient ^{137}Cs decayed between Year 70 and 80 that the amount present in the vapor decreased slightly. As in the storage temperature case, the vaporization followed the typical relationship expected for thermally driven vaporization, as shown in Figure 8.

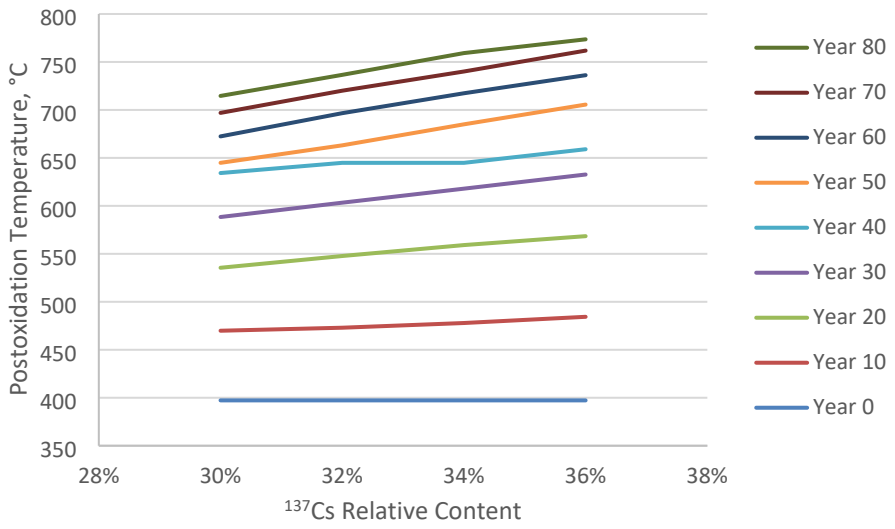

Figure 6. Adiabatic temperature achieved from thermodynamic equilibrium calculations as a function of Cs isotopic content.

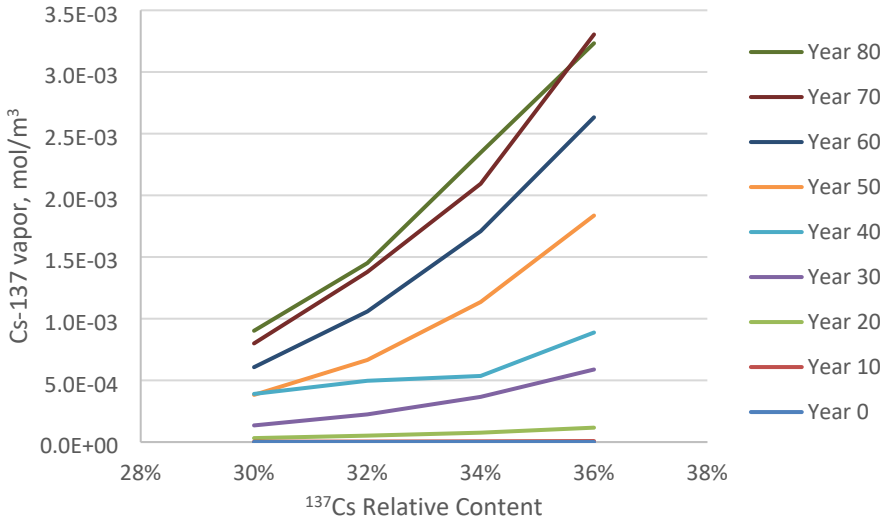

Figure 7. Cesium-137 vapor concentration achieved as a function of initial isotopics from thermodynamic equilibrium calculations.

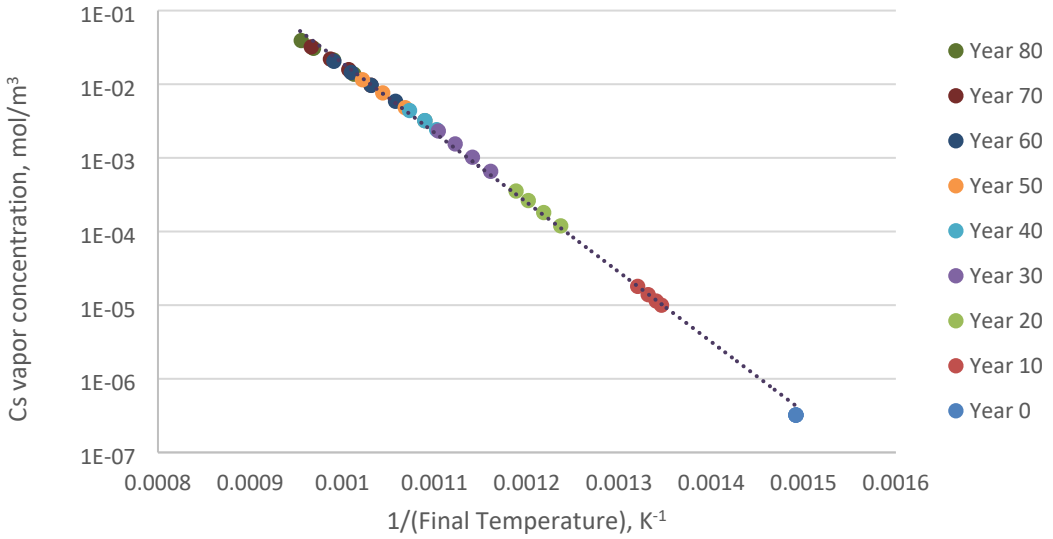

Figure 8. Cesium vapor concentration as a function of inverse temperature for variations in initial cesium isotopics.

4.3 EFFECT OF IMPURITIES

The effect of variations in impurity concentration had varied effects on the final temperature and ^{137}Cs vapor concentration. These effects can generally be grouped into three categories with respect to the final temperature and ^{137}Cs vapor concentration: increasing, decreasing, and having a minimal effect. The categories are summarized in Table 11 and are discussed individually in the following subsections.

Table 11. Categorization of impurity effects on the final adiabatic temperature and Cs vaporization potential.

Increasing Effect	Decreasing Effect	Minimal Effect
Ti, Mg	B, Ca, Cr, K, Mo, Na, Ni, Pb, Rb, Si	Zr, Sr, Mo, Mn, Fe, Cu

4.3.1 Increasing Effects

Both Ti and Mg had very minor increases in the final achieved temperature and the Cs vaporization potential, with Ti having a larger effect. The effect in Ti appears to be related to the oxidation of the original Ti chloride to form Ti oxides, which increases the overall temperature. For Mg, the oxidation of the chloride also appears to be the driver; however, the primary Mg-containing end product is the borate MgB_4O_7. The effect due to Mg was only evident in young capsules and was not significant over age 70. Unfortunately, the combined effect of the B and Mg content was not examined in this study. The same general thermally-driven vaporization observable in Figure 5 and Figure 8 was also observable for both Ti and Mg.

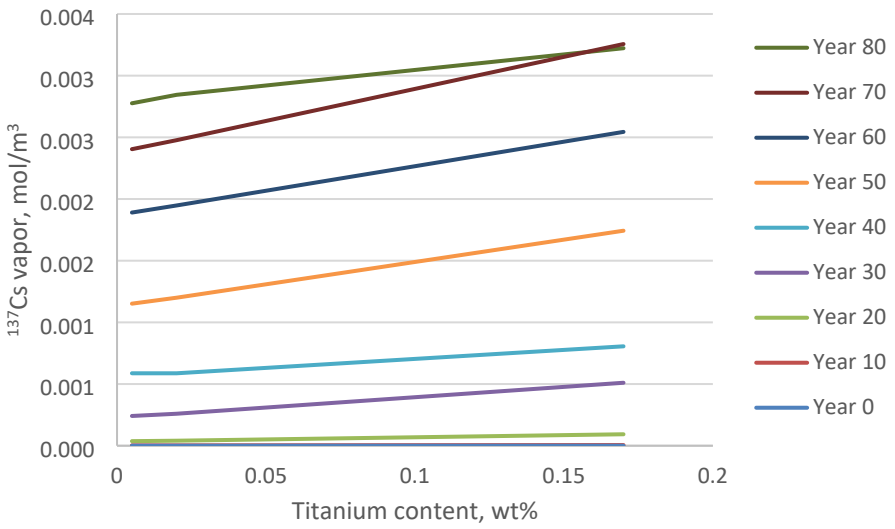

Figure 9. Effect of Ti content on potential ^{137}Cs vapor concentration.

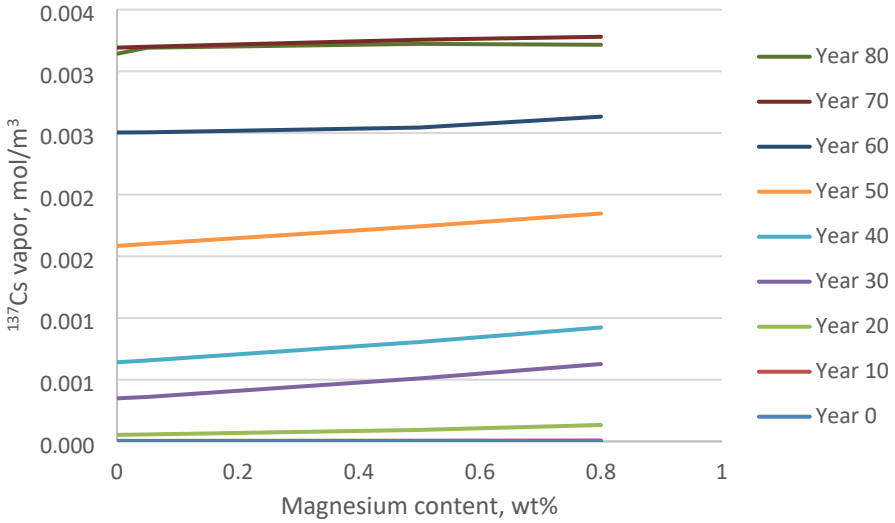

Figure 10. Effect of Mg content on potential ^{137}Cs vapor concentration.

4.3.2 Decreasing Effects

The majority of impurities decrease the final adiabatic temperature and ^{137}Cs vaporization potential. The extent of the effect and the apparent mechanism of the effect vary considerably and are difficult to compare within the current study. The largest reduction effect was seen in B, Na, and Si impurities. However, Na and Si are not strongly reactive in the simulation, with Na remaining as NaCl and Si partially combining with Zr to form $ZrSiO_4$ and partially remaining in the original SiO_2 form. These impurities appear to induce the reduction simply by displacement of the original CsCl material—because they are present in such high quantities at the high end of their range, the amount of CsCl material is significantly reduced, and thus the reaction with O has less of an effect relative to the overall thermal mass of the system. Introduced to the system as B_2O_3, B is strongly reactive with many other impurities, including Na, Mg, Mo, Pb, and Al. The lower ends of its range show these effects and provide a typical

thermal-driven vaporization behavior. However, at the highest end of its range, not enough other impurities exist to react with it, and the B primarily stays as B_2O_3, which liquifies within the temperature ranges achieved by the reaction. Between the liquefaction of B_2O_3 and simple displacement, the vaporization of Cs essentially vanishes at the highest quantities of B. The effect from B_2O_3 is presented in Figure 11.

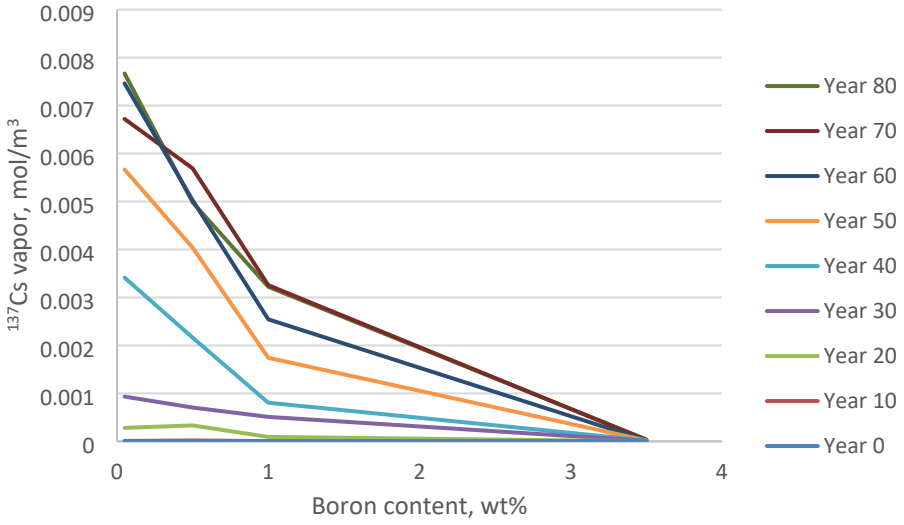

Figure 11. Cesium-137 vapor concentration potential as a function of boron content.

The other major mechanism is the tendency of impurities to lower the impact of decay. As Ba grows into the system, it reduces impurity chlorides, which in turn release less heat upon oxidation of the reduced metal. However, this effect was inconsistent because some of the species that reduce readily (Cr, Mo, Ni, Pb) decrease the vaporization potential, and others (Fe, Cu) have minimal effect. The effect from Ni is shown in Figure 12 as an example.

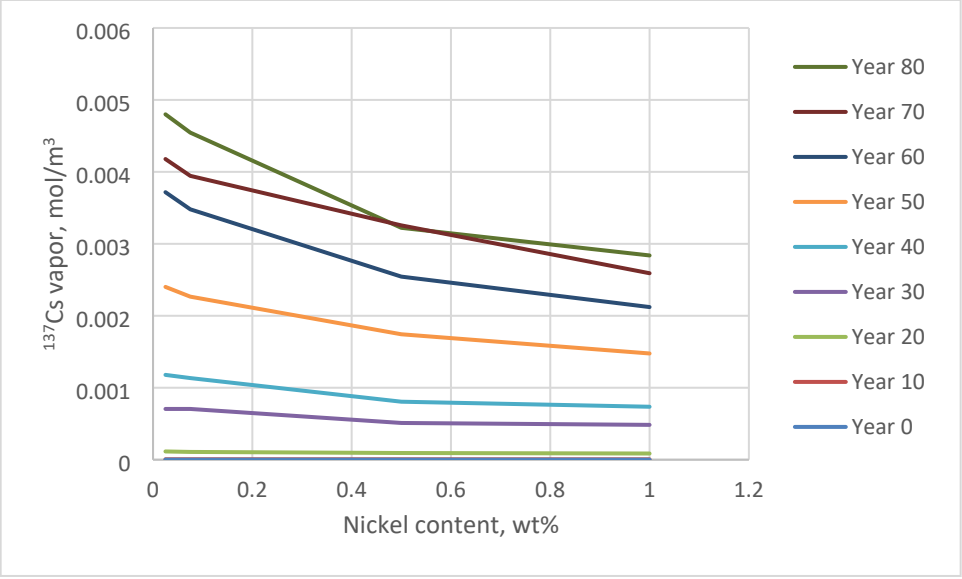

Figure 12. Cesium-137 vapor concentration potential as a function of nickel content.

The primary mechanism by which impurities reduce the potential vapor pressure of the system is by displacing the quantity of ^{137}Cs that gets loaded into the capsule, which both reduces the amount of Ba that grows into the system over time for the same amount of thermal mass, reducing the temperature of the system and thus the amount of thermally driven vaporization.

4.3.3 Minimal Effect

The variation of impurities Zr, Sr, Mo, Mn, Fe, and Cu had minimal effect on the final adiabatic temperature and Cs vaporization potential. For Zr, Mn, and Sr, these species are generally chemically unaffected by exposure to atmospheric O. Zirconium removes O from other species inside the sealed capsule and is thus already oxidized before it is breached. Other elements (Mn, Sr) remain as chlorides and are unaffected by exposure to O; thus, they do not contribute to the heat generated. For Mo and Cu, the impurity ranges are very narrow, so their contribution to the oxidation heat is very small.

The main mechanism for Fe effects is not fully clear. Although Fe is present over an impurity range comparable with Ni and is relatively easy to reduce, in the simulation it formed complex chlorides $KFeCl_3$ and K_2FeCl_4 with K, which are only oxidized at high temperatures. This appeared to flatten the ability of Fe to buffer the oxidation heat. The overall behavior of Fe is shown in Figure 13.

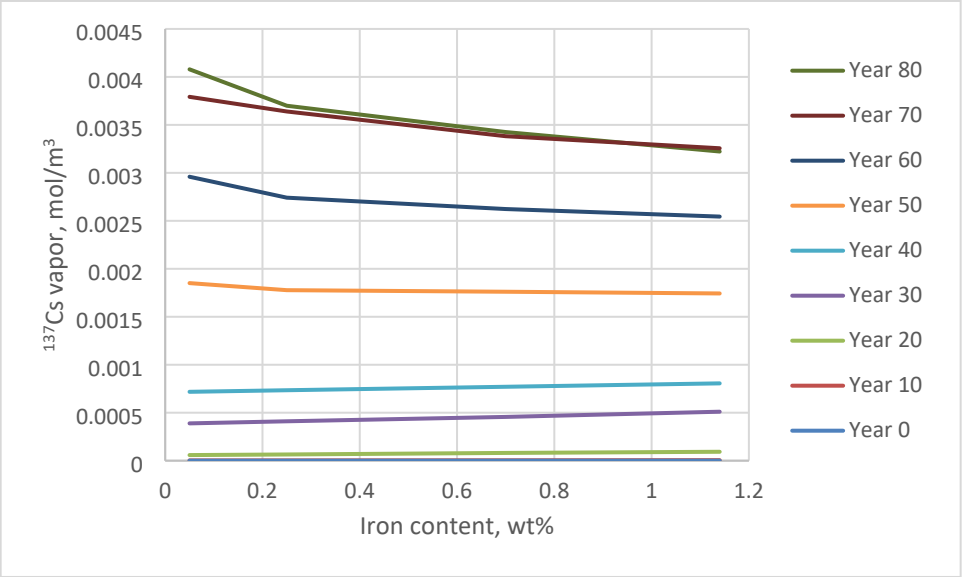

Figure 13. Cesium-137 vapor concentration potential as a function of iron impurity content.

5. SUMMARY AND CONCLUSIONS

The behavior of CsCl sealed sources has been examined and indicates a strong possibility that ^{137}Cs could be vaporized if contents were exposed to atmospheric oxygen. The study is based completely on calculations of equilibrium chemistry to simulate internal conditions and the possibilities for rapid oxidation and vaporization from exposure to O_2. The mechanism for vaporization is based on increased temperature due to exothermic reactions; formation of more volatile Cs species plays a negligible role. The decay of ^{137}Cs to ^{137}Ba is a primary contributor to reducing conditions inside typical capsules and increases over time. However, calculations indicated that even before any decay, a strong exothermic reaction would convert some of the chloride impurities to oxides, vaporizing some of the CsCl contents in the process. The study considered the effects of impurity contents, varying Cs isotopics, storage temperature, and decay time in assessing the possibilities for ^{137}Cs vaporization. Because the evaluations

in this study are all based on equilibrium calculations, they may represent worst-case scenarios. No assurance exists that kinetics of the rapid oxidation would occur completely or quickly enough to produce the serious vaporization events. Using reaction kinetics and heat conduction, the ability of the capsule to transfer heat to surroundings before reaching its maximum temperature could be investigated. However, the overall conclusion of the work is that a strong possibility exists for rapid oxidation and vaporization of ^{137}Cs, and safe handling and dismantlement of such sources should take this into account.

6. REFERENCES

1. S. N. Storch, *Characteristics of Cesium and Strontium Source Materials from the Hanford Waste Encapsulation and Storage Facility Used for Source Fabrication at Oak Ridge National Laboratory*, ORNL/TM-2005/217, Oak Ridge National Laboratory (July 2006).
2. R. O. Hultgren, *Cesium-137: A Systems Evaluation, Encapsulation to Release at Radiation Sterilizers, Inc. Decatur Georgia*, Interim Report of the DOE Type B Investigation, DOE/ORO-914 (July 1990).
3. J. M. Tingey, M. G. Plys, G. L. Tingey, *Capsule Integrity Report for Capsule Dry Storage Project*, WMP-16939, Fluor Hanford (2003).
4. National Nuclear Security Administration and Triad National Security, LLC, *Sealed Source Recovery at the University of Washington Harborview Training and Research Facility Results in Release of Cesium-137 on May 2, 2019*, Joint Investigative Report, T. Wyka, Cognizant Secretarial Officer for Safety (March 30, 2020).
5. C. W. Bale et al., "FactSage Thermochemical Software and Databases, 2010–2016," *CALPHAD* **54**, 35–53 (2016).
6. E. Lamb, *Cesium-137 Source Material for an Irradiator*, CONF-800964-1. Presented at the National Symposium on the Use of Cesium-137 to Process Sludge for Further Reduction of Pathogens, Denver, Colorado, USA, September 3, 1980.
7. C. Jiang, C. R. Stanek, N. A. Marks, K. E. Sickafus, and B. P. Uberuaga, "Predicting from First Principles the Chemical Evolution of Crystalline Compounds Due to Radioactive Decay: The Case of the Transformation of CsCl to BaCl," *Phys. Rev. B* 79, 132110 (2009).
8. B. P. Uberuaga, C. Jiang, C. R. Stanek, K. E. Sickafus, N. A. Marks, D. J. Carter, and A. L.Rohl, "Implications of Transmutation on the Defect Chemistry in Crystalline Waste Forms," *Nucl. Inst. and Methods in Phys. Res. B* 268, 3261-4 (2010).
9. H. T. Fullam, *Cesium Chloride Compatibility Testing Program Annual Report – Fiscal Year 1982*, PNL-4556 (UC-70), Pacific Northwest Laboratory (December 1982).
10. G. H. Bryan, *Cesium Chloride Compatibility Testing Program – Final Report*, PNL-7133 (UC-721) Pacific Northwest Laboratory (November 1989).
11. G. H. Bryan, G. L. Tingey, and D. R. Olander, *Corrosion Report for Capsule Dry Storage*, WMP-16937, Fluor Hanford (2003).
12. B. T. Kenna and F. J. Schultz, *Characterization of an Aged WESF Capsule*, SAND83-0928, Sandia National Laboratory (July 1983).
13. R. R. Jackson, "Hanford Waste Encapsulation: Strontium and Cesium," *Nucl. Tech* 32:10–15 (1977).
14. D. J. Sasmor, J. D. Pierce, G. L. Tingey, H. E. Kjarmo, J. Tills, and D. C. McKeon, *Characterization of Two WESF Capsules After Five Years of Service*, SAND86-2808, Sandia National Laboratory (April 1988).

15. G. L. Tingey, E. J. Wheelwright, J. M. Lytle, *A Review of Safety Issues that Pertain to the Use of WESF Cesium Chloride Capsules in an Irradiator*, PNL-5170 (UC-70), Pacific Northwest Laboratory (July 1984).

16. I. Urieli, *Engineering Thermodynamics – A Graphical Approach*, Ohio University, (updated March 2021), https://www.ohio.edu/mechanical/thermo/property_tables/combustion.

APPENDIX A. IMPURITY DISTRIBUTIONS

As noted previously, many measurements have been undertaken by numerous researchers to characterize the impurity contents of Waste Encapsulation and Storage Facility (WESF) capsules. These have been ordered and appear for the important impurities in Table A.1. Note that some impurities are measured frequently and some only a few times. Impurities not listed may have been occurred in a few reports, but they were present in very small amounts (if at all) and would therefore not pose a major impact on the redox conditions inside the capsules. Hence, they were not included in the analyses of this report.

Table A.1. Impurity measurements in WESF capsules. BDL=below detection limit

Al	BDL	BDL	BDL	BDL	BDL	BDL	0.05	0.1	0.1	0.1	0.14	0.2	0.21	0.3
	0.68	1.7	2.7											
B	BDL	BDL	BDL	0	0.01	0.02	0.03	0.04	0.14	0.3	0.4	0.5	5.17	
Ca	0.01	0.01	0.02	0.02	0.02	0.03	0.05	0.05	0.06	0.19	0.3	0.4	0.68	1
Co	0.02	0.1												
Cr	BDL	0.02	0.05	0.05	0.06	0.1	0.1	0.1	0.1	0.2	0.27	0.3	0.5	1.4
Cu	BDL	0.02	0.03	0.2										
Fe	BDL	0.04	0.04	0.09	0.1	0.2	0.2	0.2	0.2	0.38	0.5	0.8	1.6	2.1
	4	high												
K	BDL	BDL	BDL	BDL	BDL	0.07	0.09	0.1	0.18	0.2	0.6	0.68	0.7	0.7
	0.79	1.21	9.2											
Mg	BDL	BDL	BDL	BDL	BDL	0	0.01	0.01	0.04	0.05	0.05	0.1	0.25	0.6
Mn	BDL	BDL	BDL	0.01	0.01	0.01	0.02	0.04	0.05	0.05	0.09			
Mo	BDL	BDL	BDL	BDL	0.01	0.05	0.06	0.06	0.26					
Na	0.04	0.1	0.1	0.1	0.18	0.2	0.2	0.3	0.3	0.3	0.3	0.7	0.7	1.5
	2.8	4.5	7.76											
Ni	BDL	BDL	0.02	0.02	0.05	0.06	0.06	0.08	0.09	0.1	0.1	0.1	0.16	0.2
	0.33	1.5												
Pb	BDL	BDL	0.11	0.14	1.4									
Rb	BDL	0.02	0.05	0.06	0.1	0.52	1.5							
Si	BDL	BDL	BDL	BDL	BDL	BDL	BDL	BDL	0.04	0.1	0.2	0.21	2.59	5
	7													
Sr	BDL	BDL	BDL	BDL	BDL	BDL	BDL	BDL	0	0.01	0.01	0.02	0.05	0.18
Ti	BDL	BDL	BDL	0.02	0.02	0.03	0.03	0.04	0.07					
Zr	BDL	BDL	BDL	BDL	0.01	0.02	0.04	0.04	0.04					

The above values (including the BDL values) were combined into histogram-based distributions similar to Table 1 and Figure 1. These distributions are described in Table A.2, where the values x_i delineate the different histogram regions, with $x_0 = 0$, and x_i as noted in the table for each element. The value of x_4 (in some cases x_3) is the maximum allowed for that element. Columns 6–9 represent cumulative probabilities related to the regions bounded by x_i as an upper bound. These probabilities are derived from the integer numbers of occurrences in Table A.1 for those respective regions. For the Na example in Table 1 and Figure 1, there are 17 total measurements, and within the four histogram regions, the numbers of occurrences (see Table 1) are 4, 7, 3, and 3, respectively. Therefore, the probabilities in each region are:

$$P_1 = \frac{4}{17}, \quad P_2 = \frac{7}{17}, \quad P_3 = \frac{3}{17}, \quad P_4 = \frac{3}{17},$$

and the cumulative probabilities are

$$\Pr(X \le x_1) = \frac{4}{17} = 0.235, \quad \Pr(X \le x_2) = \frac{4}{17} + \frac{7}{17} = 0.647, \quad \Pr(X \le x_3) = \frac{14}{17} = 0.824\,.$$

Since x_4 is the upper limit for each distribution, then $\Pr(X \le x_4) = 1$ in every case.

Table A.2. Distributions of Impurities.

	x_1	x_2	x_3	x_4	$\Pr(X \le x_1)$	$\Pr(X \le x_1)$	$\Pr(X \le x_1)$
Al	0.05	0.15	0.5	3	0.352941	0.647059	0.823529
B	0.01	0.1	1	6	0.307692	0.615385	0.923077
Ca	0.03	0.1	0.5	3	0.461538	0.692308	0.923077
Cr	0.1	0.2	0.4	4.27	0.357143	0.642857	0.857143
Cu	0.01	0.1	0.3	1	0.25	0.75	1
Fe	0.1	0.4	1	5	0.25	0.625	0.75
K	0.1	0.4	0.8	1.5	0.411765	0.588235	0.882353
Mg	0.01	0.1	0.5	1	0.5	0.785714	0.928571
Mn	0.01	0.03	0.06	0.11	0.454545	0.636364	0.909091
Mo	0.01	0.04	0.1	0.26	0.555556	0.555556	0.888889
Na	0.1	0.5	2	8	0.235294	0.647059	0.823529
Ni	0.05	0.1	0.5	1.5	0.25	0.5625	0.9375
Pb	0.1	0.5	2	10	0.4	0.8	1
Rb	0.02	0.1	1	1.5	0.142857	0.571429	0.857143
Si	0.01	0.1	1	7	0.533333	0.6	0.8
Sr	0.001	0.01	0.1	0.3	0.571429	0.714286	0.98571
Ti	0.01	0.03	0.1	1	0.333333	0.777778	1
Zr	0.01	0.03	0.1	1	0.444444	0.666667	1

APPENDIX B. SENSITIVITY STUDIES

The following tables indicate the conditions used for calculating the relationships obtained during the sensitivity studies. Values were based on the reports for capsule C-117 from the report by Storch [1]. For Al, the presumed source of Al impurities is expected to be the ion exchange resin during the Cs purification, which would presumably be in the form of Al and Si oxides and is reported by Storch to be either in the form $AlCl_3$ or the form Al_2SiO_5. However, in trying to modify the values for the starting conditions, mass and charge balance had to be maintained. A variable was introduced and fitted to allow switching between Al_2SiO_5 and $AlCl_3/SiO_2$ as the source of Si while trying to solve the anion balance, and this variable always fitted to 100% $AlCl_3/SiO_2$ to close the anion balance. Therefore, Al was introduced into the system as the chloride and not the oxide.

Table B.1. Baseline conditions for sensitivity studies.

Temperature = 168.5°C, Cs-137 = 32% of Cs isotopes, 27.08 total moles	
Solid Phase Impurities	**Weight %**
Al (as $AlCl_3$)	0.7
B (as B_2O_3)	1.0
Ca (as $CaCl_2$)	0.2
Co (as $CoCl_2$)	0.22
Cr (as $CrCl_3$)	1.0
Cu (as CuCl)	0.31
Fe (as $FeCl_2$)	1.14
K (as KCl)	1.51
Mg (as $MgCl_2$)	0.5
Mn (as $MnCl_2$)	0.11
Mo (as $MoCl_5$)	0.06
Na (as NaCl)	2.0
Ni (as $NiCl_2$)	0.5
Pb (as $PbCl_2$)	1.0
Rb (as RbCl)	0.7
Si (as SiO_2)	0.9
Sr (as $SrCl_2$)	0.33
Ti (as $TiCl_2$)	0.17
Zr (as $ZrCl_4$)	0.20
Gas Phase Impurities	Moles
H_2	9.4×10^{-7}
He	1.059×10^{-3}
CH_4	2.45×10^{-7}
H_2O	2.86×10^{-6}
N_2 + CO (as N_2)	4.66×10^{-4}
O_2	8.17×10^{-8}
Ar	7.68×10^{-4}
CO_2	1.14×10^{-6}

Table B.2. Modifications from baseline for sensitivity studies.

Test No.	Modification of Run Conditions from Baseline
1	Baseline
2	Initial Temp. = 120.667°C
3	Initial Temp. = 72.833°C
4	Initial Temp. = 25°C
5	Cs-137 = 30%
6	Cs-137 = 34%
7	Cs-137= 36%
8	Cs-137= 36%, Al = 0.325 wt%
9	Cs-137= 36%, Al = 0.1 wt%
10	Cs-137= 36% Al = 0.025 wt%
11	Cs-137= 36%, B = 3.5 wt%
12	Cs-137= 36%, B = 0.5 wt%
13	Cs-137= 36%, B = 0.05 wt%
14	Cs-137= 36%, B = 0.005 wt%
15	Cs-137= 36%, Ca = 1.635 wt%
16	Cs-137= 36%, Ca = 0.065 wt%
17	Cs-137= 36%, Ca = 0.015 wt%
18	Cs-137= 36%, Cr = 0.3 wt%
19	Cs-137= 36%, Cr = 0.15 wt%
20	Cs-137= 36%, Cr = 0.05 wt%
21	Cs-137= 36%, Cu = 0.05 wt%
22	Cs-137= 36%, Cu = 0.005 wt%
23	Cs-137= 36%, Fe = 0.7 wt%
24	Cs-137= 36%, Fe = 0.25 wt%
25	Cs-137= 36%, Fe = 0.05 wt%
26	Cs-137= 36%, K = 0.6 wt%
27	Cs-137= 36%, K = 0.2 wt%
28	Cs-137= 36%, K = 0.05 wt%
29	Cs-137= 36%, Mg = 0.8 wt%
30	Cs-137= 36%, Mg = 0.05 wt%
31	Cs-137= 36%, Mg = 0.0005 wt%
32	Cs-137= 36%, Mn = 0.045 wt%
33	Cs-137= 36%, Mn = 0.02 wt%
34	Cs-137= 36%, Mn = 0.005 wt%
35	Cs-137= 36%, Mo = 0.045 wt%
36	Cs-137= 36%, Mo = 0.02 wt%
37	Cs-137= 36%, Mo = 0.005 wt%
38	Cs-137= 36%, Na = 5 wt%
39	Cs-137= 36%, Na = 0.3 wt%
40	Cs-137= 36%, Na = 0.05 wt%

Table B.2. Modifications from Baseline for Sensitivity Studies (continued).

Test No.	Modification of Run Conditions from Baseline
41	Cs-137= 36%, Ni = 1 wt%
42	Cs-137= 36%, Ni = 0.075 wt%
43	Cs-137= 36%, Ni = 0.025 wt%
44	Cs-137= 36%, Pb = 0.3 wt%
45	Cs-137= 36%, Pb = 0.05 wt%
46	Cs-137= 36%, Rb = 1.25 wt%
47	Cs-137= 36%, Rb = 0.05 wt%
48	Cs-137= 36%, Rb = 0.005 wt%
49	Cs-137= 36%, Si = 4 wt%
50	Cs-137= 36%, Si = 0.05 wt%
51	Cs-137= 36%, Si = 0.005 wt%
52	Cs-137= 36%, Sr = 0.05 wt%
53	Cs-137= 36%, Sr = 0.005 wt%
54	Cs-137= 36%, Sr = 0.0005 wt%
55	Cs-137= 36%, Ti = 0.02 wt%
56	Cs-137= 36%, Ti = 0.005 wt%
57	Cs-137= 36%, Zr = 0.02 wt%
58	Cs-137= 36%, Zr = 0.005 wt%